Supporting Information

Vaeth et al. 10.1073/pnas.1203870109

SI Materials and Methods

Mice and Cells. *Nfat2*$^{fl/fl}$ (nuclear factor of activated T-cells) animals were generated in A. Rao's laboratory (Harvard Medical School, Boston, MA). Nfat1$^{-/-}$ × Nfat4$^{-/-}$, B6-Tg (Cd4-cre) 1Cwi/Cwilbcm (European mouse mutant archive, Rome, Italy) and Foxp3-IRES-cre have been described previously (1–3). Animals were used at 6–16 wk and maintained in accordance with institutional guidelines for animal welfare. Blood from healthy donors was obtained after informed consent, in accordance with the Declaration of Helsinki, under a protocol that received approval from the Institutional Review Board from the Johannes Gutenberg university hospital in Mainz.

Antibodies, Reagents, and Media. mAbs against CD3ε (145-2C11), CD28 (37.51; both BD Pharmingen), and CD4 (YTS177.9; Bio-Xcell), as well as superagonistic CD28 mAb D665 (CD28SA; Serotec), were used as previously described (4). Recombinant hIL-2 (50 U/mL), hIL-6 (50 ng/mL), mIL-12 (10 ng/mL), hIL-21 (65 ng/mL), mIFN-γ (50 ng/mL), hTGF-β1 (1–5 ng/mL), and mIL10 (20 ng/mL; all PeproTech), anti-IL-2 (5 μg/mL; eBioscience), anti-IL-4 and anti-IFNγ (both 2.5 μg/mL; R&D Systems), 5 12-*O*-tetradecanoyl-phorbol-13-acetate (TPA, 10 ng/mL; Sigma), ionomycin (5 nM; Merck Biosciences), and cyclosporin A (CsA; Calbiochem) were used as indicated. CD4$^+$ T cells were cultivated in RPMI 1640 (5, 6).

Preparation of T-Cell subsets. Human T-cell subsets were isolated and stimulated as shown previously (7, 8). Murine CD4$^+$CD25$^+$ naturally occurring regulatory T cells (nTreg) and CD4$^+$CD25$^-$ conventional naïve CD4$^+$ T cells (Tconv) were isolated (6) using Dynal Mouse T Cell Negative Isolation Kit (Invitrogen) followed by staining with anti-CD25-PE mAb and anti-PE MACS beads enrichment (Miltenyi Biotech).

Cell Culture and Stimulations. Priming and restimulation of primary T cells was performed using plate-bound anti-CD3 mAb (145-2C11, 5 μg/mL) plus anti-CD28 mAb (37.51, 1 μg/mL) (both BD Pharmingen). After 72 h the cells were washed and cultured on fresh plates for additional 96 h. For intracellular cytokine analysis cells were stimulated for 6 h with TPA/Iono in presence of GolgiPlug and GolgiStop (both BD Pharmingen).

FACS Staining. FACS staining (6) was carried out with the following Ab: fluorescein isothiocyanate (FITC)-conjugated CD4 (GK1.5), CD8α (53-6.7), CD19 (1D3), GITR (DTA-1); phycoerythrin (PE)-conjugated CD3ε (145-2C11), CD4 (RM4-5), CD19 (1D3), CD25 (PC61), CD39 (24DMS1), CD73 (eBioTY/11.8) CD103 (2E7), CD107a (eBio1D4B), OX-40 (OX-86), Lag3 (eBioC9B7W), CTLA-4 (UC10-4B9); allophycocyanin (APC)-conjugated CD8α (53-6.7); eFluor710-conjugated GARP (YGIC86) and LAP (TW7-16B4); biotin-conjugated CD3ε (145-2C11), CD4 (GK1.5), and CD90.2 (53-2.1), and secondary streptavidin-HRP, streptavidin-APC or streptavidin-PE mAb (all BD Pharmingen). Intracellular Foxp3 (FJK-16s, FITC-, PE-, and APC-conjugated), Helios (22F6, FITC-conjugated, BioLegend), and cAMP (SPM486, Abcam), together with donkey-anti-mouse-AlexaFluor555 (Invitrogen), staining was performed using the Foxp3 staining kit (eBiosciences). Cytokine staining for IL-2-APC (JES6-5H4), IFN-γ–APC (XMG1.2), IL-17-PE (eBio17B7), and TNFα-PE (MP6-XT22) was performed using the IC Fixation Buffer Kit (eBioscience). Samples were analyzed on a FACS Calibur (BD Biosciences) with CellQuest (BD Biosciences) and FlowJo software (TreeStar).

ELISA. Cells (1 × 10^6/mL) were cultivated as indicated for 48 h. The supernatant was analyzed by IL-2 ELISA (eBiosciences).

Calcium Measurement. Splenic CD4$^+$ T cells (1 × 10^7) were incubated in medium containing 5% (vol/vol) FCS, 1 μM Indo-1-AM (Invitrogen), and 0.015% Pluronic F127 (Invitrogen) at 30 °C for 25 min. The cell suspension was then diluted with 700 μL medium containing 10% (vol/vol) FCS and incubated at 37 °C for another 10 min. The cells were washed twice with PBS followed by surface staining with anti-CD4-PacificBlue, anti-CD25-PE, and biotinylated anti-CD3ε (all eBioscience). For calcium measurement, cells were diluted 1:10 in PBS containing 0.5 mM EGTA, and a baseline was recorded for 60 s. Ca^{2+} movement was assessed after streptavidin-HPR cross-linking (eBioscience), followed by the addition of 1 mM Ca^{2+} after 3.5 min and Iono after 9 min of recording. After 12 min, another baseline of unstimulated cells was recorded as control. Increases in free intracellular Ca^{2+} were measured in real-time on an LSR II (BD), and data were analyzed as median in comparative overlays with FlowJo software (TreeStar).

Proliferation Assays. Proliferation assay (6) was measured using a Mach 2 Harvester (Tomtec).

Immunofluorescence. For confocal microscopy (5, 6) the following primary antibodies were used: anti-NFAT2 (7A6; BD Pharmingen), anti-NFAT1 (IG-209; immunoGlobe), anti-Smad3 (ab28379; Abcam), and anti-Foxp3 (FJK-16s; eBiosciences). Secondary staining was performed using Abs: anti-rabbit Alexa-Fluor 647, anti-mouse Alexa-Fluor 488, and anti-rat Alexa-Fluor 555 (all Molecular Probes). Slides were mounted with Fluoromount-G (Southern Biotechnology) containing DAPI. Images were taken with a confocal microscope (Leica TCS SP2 equipment, objective lense; HeX PL APO, 40×/1.25–0.75) and LCS software (Leica). For statistics, more than 100 cells from at least three independent experiments were counted, and mean fluorescence intensity per cell was calculated.

Immunoblot. Protein lysate was made with radioimmunoprecipitation assay buffer (RIPA) buffer and measured using bicinchoninic acid (BCA) reagent (BioRad). Equal amount of protein was fractionated by 8–12% SDS/PAGE and electroblotted on membranes (5). For detection, anti-NFAT2 (7A6; BD Pharmingen), anti-NFAT1 (IG-209; immunoGlobe), anti-NFAT4 (F-1; Santa Cruz Biotechnology), and anti-β-actin (C4; Santa Cruz Biotechnology) with anti-mouse or anti-rabbit peroxidase-coupled secondary antibodies were used.

PCR and Quantitative RT-PCR. Genomic DNA was prepared with DNA-lysis buffer (including 0.2% SDS). PCR was performed using the following primers (5′→3′): *Nfat2* CCTATTTAAACACCTGGCTCCCTGCG plus CCATCTCTCTGACCAACAGAAGCC AG, Δexon3 CTAGGCCTCAGGCGTTCCACC plus CCTGCCTCTCTCAGCCTTTGA, *Cebp* CGAGCCACCGCGTCCTCCAGC plus CCGGTCGGTGCGCGTCATTGC. RNA was extracted using the RNeasy Micro Kit (Qiagen) followed by cDNA synthesis which was performed with the iScript II Kit (BioRad). Real-time quantitative RT-PCR was carried out with an ABI Prism 7700 detection system using the following primers: *Nfat1* TCATAGGAGCCCGACTGATTG plus CCATTCC-

CATCTGCAGCAT, *Nfat2* GATCCGAAGCTCGTATGGAC plus AGTCTCTTTCCCCGACATCA, *Nfat4* CACATCCCACAGCCCAGTG plus CACATCCCACAGCCCAGTG normalized to *β-actin* GACGGCCAGGTCATCACTATTG plus AGGAAGGCTGGAAAAGAGCC.

ChIP Analysis. ChIP-IT Express kit (Active Motif) was used according to the manufactures' instructions, except for enzymatic shearing followed by additional sonication. The following IP-Abs were used: anti-NFAT2 (7A6; BD Pharmingen), anti-Foxp3 (FJK-16s; eBioscience), and anti-Smad3 (Abcam). Primers (5′→3′) used were: Foxp3-Pr CTTCCCATTCACATGGCAGGC plus CTTTGCCCTTTACAAGTCATCTG; Foxp3-CNS1 GCACTTGAAAATGAGATAACTGTTC plus CATCACAGTACATACGAGGAAATG; and Foxp3-CNS3 CCAGATGGACGTCACCTACC plus GGCGTTCCTGTTT-GACTGTTTC.

Electromobility Shift Assay (EMSA). Nuclear proteins from human and murine T-cell subsets were prepared and stored by ProteoJET Kit (Thermo Scientific). *hFoxp3-Prom-NFAT* GTTCT**TCTTCC**TTGTTTTTTTTT; *mFoxp3-Prom-NFAT* GACTTA**TTTTCC**CTCAGTTTTTTTTTT; *mFoxp3-CNS1-NFAT* GCTTCATT**TTTTCC**ATTTACTG; *mIL2-Pubd* CCCCAAAGA**GGAAA**ATTTGTTT (boldface, NFAT consensus sites); anti-NFAT1 (D43B1, Cell Signaling), and anti-NFAT2 (7A6, BD Pharmingen) were used for EMSA, which was performed as previously described (9).

Microarray. $CD4^+CD25^+$ nTregs and $CD4^+CD25^-$ Tconv from WT or *Nfat1*$^{-/-}$ × *Nfat2*$^{fl/fl}$ × *Cd4-cre* (DKO) mice were isolated and stimulated for 24 h with plate-bound anti-CD3/28 in absence (Tconv and nTreg) or presence (iTreg conditions) of 5 ng/mL TGF-β, followed by RNA extraction using the standard TRIzol method (Invitrogen). Biotin-labeled amplified aRNA was prepared using the GeneChip 3′ IVT Express Kit and hybridized to GeneChip mouse genome 430 2.0 arrays (Affymetrix) according to the manufacturer's protocols. The trimmed mean signals of the probe arrays were scaled to a target value of 500 and expression values determined using Affymetrix GeneChip Operating Software. Data were analyzed and visualized as a heat map using GeneSpring GX 12.0 software (Agilent Technologies). The original microarray data can be found in the ArrayExpress database under the accession no. E-MEXP-12345 (www.ebi.ac.uk/arrayexpress).

CD28SA Treatment. Treatment of mice with superagonistic CD28 mAb D665 was performed as previously described (4). Mice received a single i.p. injection of 250 μg CD28SA D665 (Serotec) or PBS as control. After 60 h serum samples were obtained from tail vein. Spleen and LN cells were harvested on day 3 post injection.

Adoptive Transfer Colitis and Endoscopy. Colitis was induced in *Rag1*$^{-/-}$ mice by injecting i.p. 2.5×10^5 *Cd90.1*$^+$ (WT) and 2.5×10^5 *Cd90.2*$^+$ (WT or *Nfat2*$^{fl/fl}$ × *Cd4cre*) $CD4^+CD62L^+CD25^-$ cells. Mice were anesthetized [100 μL of a mixture of 100 mg/mL Ketavest (Pfizer) and Rompun (Bayer Healthcare) i.p.] and clinical symptoms [murine endoscopic index of colitis severity (MEICS): total range 0–15 points; colon translucency (0–3 points), presence of fibrin (0–3 points), mucosa granularity (0–3 points), vascular pattern (0–3 points), and stool (0–3 points)] were analyzed with a high-resolution video endoscopic system (Karl Storz) (10).

Skin Transplant Model. To test alloantigen-induced or nTreg in vivo (11, 12) mice received 200 μg of anti-CD4 YTS177.9 mAb (Bio-Xcell) i.v. on day −28/−27. On day −27 the mice also received 250 μL donor-specific blood transfusions (DST) from BALB/c mice. $CD4^+CD25^+$ T cells were FACS-sorted on day 0, and C57BL/6 *Rag2*$^{-/-}$ mice were reconstituted i.v. with 2×10^5 C57BL/6 $CD4^+CD45RB^{hi}$ cells along with 5×10^5 $CD4^+CD25^+$ nTreg cells isolated from naïve or 2×10^5 $CD4^+CD25^+$ Treg cells from YTS177/DST-pretreated mice. Next day, BALB/c tail skin allografts were transplanted onto flanks of reconstituted mice. Graft survival between groups was monitored and compared using the log–rank test. For transfer of in vitro-generated iTregs, naïve $CD4^+$ $CD25^-$ T cells were cocultivated with BALB/c $CD19^+$ B cells in the presence of IL-2, TGF-β, anti-IL-12, anti–IFN-γ, and the anti-CD4 YTS177 for 2 wk, with restimulation after 1 wk. FACS-sorted $CD25^{hi}$ T cells were verified for Foxp3 expression, and equal numbers were used in transplantation.

Statistical Analysis. Groups were compared with Prism software (GraphPad) using two-tailed Student's *t* test.

1. Lee PP, et al. (2001) A critical role for Dnmt1 and DNA methylation in T cell development, function, and survival. *Immunity* 15:763–774.
2. Ranger AM, Oukka M, Rengarajan J, Glimcher LH (1998) Inhibitory function of two NFAT family members in lymphoid homeostasis and Th2 development. *Immunity* 9: 627–635.
3. Wing K, et al. (2008) CTLA-4 control over Foxp3+ regulatory T cell function. *Science* 322:271–275.
4. Gogishvili T, et al. (2009) Rapid regulatory T-cell response prevents cytokine storm in CD28 superagonist treated mice. *PLoS ONE* 4:e4643.
5. Nayak A, et al. (2009) Sumoylation of the transcription factor NFATc1 leads to its subnuclear relocalization and interleukin-2 repression by histone deacetylase. *J Biol Chem* 284:10935–10946.
6. Vaeth M, et al. (2011) Regulatory T cells facilitate the nuclear accumulation of inducible cAMP early repressor (ICER) and suppress nuclear factor of activated T cell c1 (NFATc1). *Proc Natl Acad Sci USA* 108:2480–2485.
7. Becker C, et al. (2009) Protection from graft-versus-host disease by HIV-1 envelope protein gp120-mediated activation of human CD4+CD25+ regulatory T cells. *Blood* 114:1263–1269.
8. Kubach J, et al. (2007) Human CD4+CD25+ regulatory T cells: proteome analysis identifies galectin-10 as a novel marker essential for their anergy and suppressive function. *Blood* 110:1550–1558.
9. Berberich-Siebelt F, et al. (2000) C/EBPbeta enhances IL-4 but impairs IL-2 and IFN-gamma induction in T cells. *Eur J Immunol* 30:2576–2585.
10. Weigmann B, et al. (2008) The transcription factor NFATc2 controls IL-6-dependent T cell activation in experimental colitis. *J Exp Med* 205:2099–2110.
11. Karim M, Kingsley CI, Bushell AR, Sawitzki BS, Wood KJ (2004) Alloantigen-induced CD25+CD4+ regulatory T cells can develop in vivo from CD25-CD4+ precursors in a thymus-independent process. *J Immunol* 172:923–928.
12. Sawitzki B, et al. (2005) IFN-gamma production by alloantigen-reactive regulatory T cells is important for their regulatory function in vivo. *J Exp Med* 201:1925–1935.

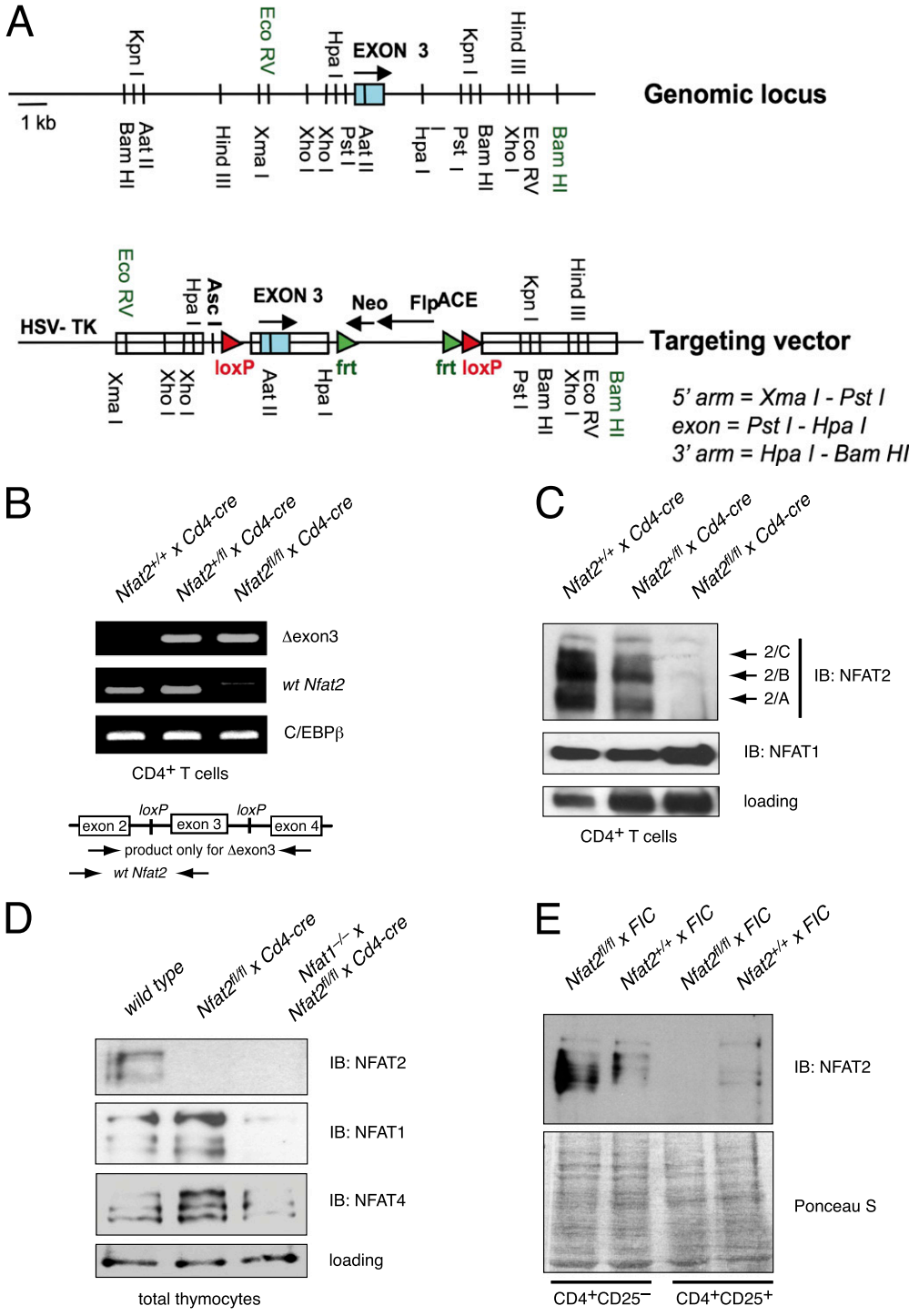

Fig. S1. Conditional disruption of *Nfat2* exon3 in mice. (A) Strategy for introduction of loxP sites into the mouse *Nfat2* locus flanking exon 3. Genomic locus of the *Nfat2* exon3 region (*Upper*) and the targeting vector containing a loxP sites flanked version of exon3 including a neomycin resistance cassette (*Lower*) bordered by frt sites. (*B* and *C*) Confirmation of conditional inactivation of *Nfat2* in $CD4^+$ T lymphocytes by CD4-mediated cre. (*B*) PCR analysis of genomic DNA of isolated $CD4^+$ T cells with specific primers for the loss of *Nfat2* exon3 (Δexon3) and total *Nfat2* (*wt Nfat2*) of WT ($Nfat2^{+/+}$ × *Cd4-cre*), heterozygous ($Nfat2^{+/fl}$ × *Cd4-cre*), and knockout ($Nfat2^{fl/fl}$ × *Cd4-cre*) mice. (*C*) Immunoblot of protein from $CD4^+$ T cells of WT, heterozygous, and homozygous mice. Arrows indicate isoforms of NFAT2. (*D*) Breeding of $Nfat2^{fl/fl}$ × *Cd4-cre* mice to $Nfat1^{-/-}$ mice resulted in NFAT1NFAT2 double-deficient T lymphocytes. Immunoblot analysis of NFAT expression in total thymocytes from WT, $Nfat2^{fl/fl}$ × *Cd4-cre*, and $Nfat1^{-/-}$ × $Nfat2^{fl/fl}$ × *Cd4-cre* mice. (*E*) Foxp3-specific inactivation of *Nfat2* in Treg cells by *Foxp3-IRES-cre* (*FIC*). Immunoblot with proteins isolated from $CD4^+CD25^-$ and $CD4^+CD25^-$ T cells of WT and $Nfat2^{fl/fl}$ × *FIC* mice.

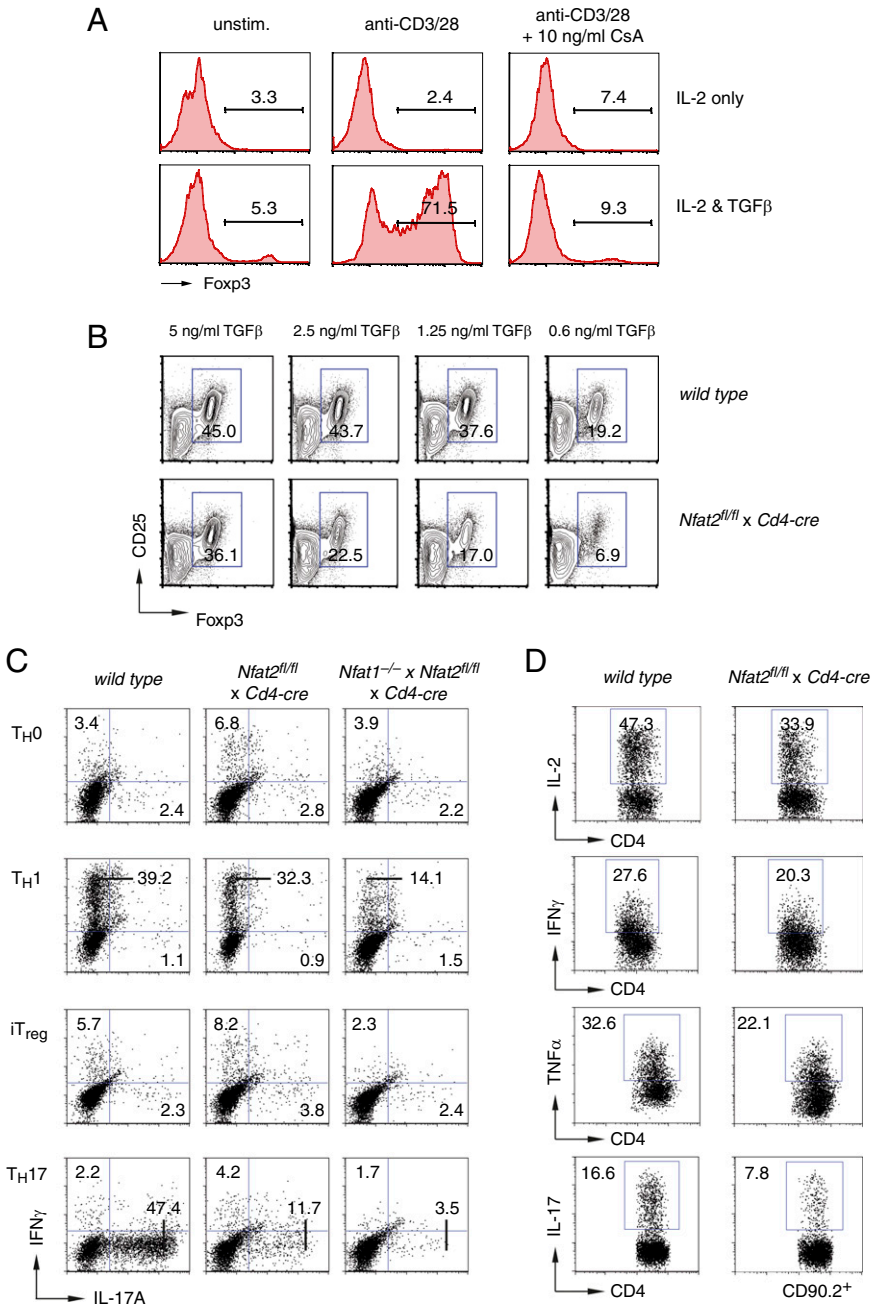

Fig. S2. Direct influence of NFAT on Foxp3 and cytokine induction. (*A*) TGF-β–mediated iTreg induction of WT $CD4^+CD25^-$ T cells is abrogated in the presence of 10 ng/mL CsA. (*B*) $CD4^+CD25^-$ T cells from WT and *Nfat2*$^{fl/fl}$ × *Cd4-cre* mice were stimulated for 3 d with plate-bound anti-CD3/28 in the presence of IL-2 and different concentrations of TGF-β, followed by rest of 4 d. Representative FACS analysis of $CD4^+CD25^+Foxp3^+$ T cells in culture. (*C* and *D*) Impaired cytokine expression in NFAT-deficient $CD4^+$ T cells. (*C*) $CD4^+CD25^-$ T cells from WT, *Nfat2*$^{fl/fl}$ × *Cd4-cre*, and *Nfat1*$^{-/-}$ × *Nfat2*$^{fl/fl}$ × *Cd4-cre* mice were cultivated for 3 d with plate-bound anti-CD3/28 under T_H0- (IL-2, anti-IL-4, anti-IFNγ), T_H1- (IL-12, IFNγ, anti-IL-4), iTreg- (IL-2, TGF-β, anti-IL-4, anti-IFNγ), and T_H17-polarizing conditions (IL-6, IL-21, TGF-β, anti-IL-4, anti-IFNγ, anti-IL-2). Cells were restimulated for 6 h with TPA/Iono followed by intracellular IFN-γ and IL-17 analysis using FACS. (*D*) Measurement of intracellular IL-2, IFN-γ, TNF-α, and IL-17 of $CD90.2^+$ WT or $CD90.2^+$ *Nfat2*$^{fl/fl}$ × *Cd4-cre* T cells transferred into *Rag2*$^{-/-}$ (lymphopenic-induced colitis, parallel to Fig. 2 *B*–*D*; Fig. S4). Total cells from mLN were stimulated for 6 h with TPA/Iono followed by intracellular FACS-staining; gating on CD4 and CD90.2 identified WT or *Nfat2*$^{fl/fl}$ × *Cd4-cre* adoptively transferred T cells.

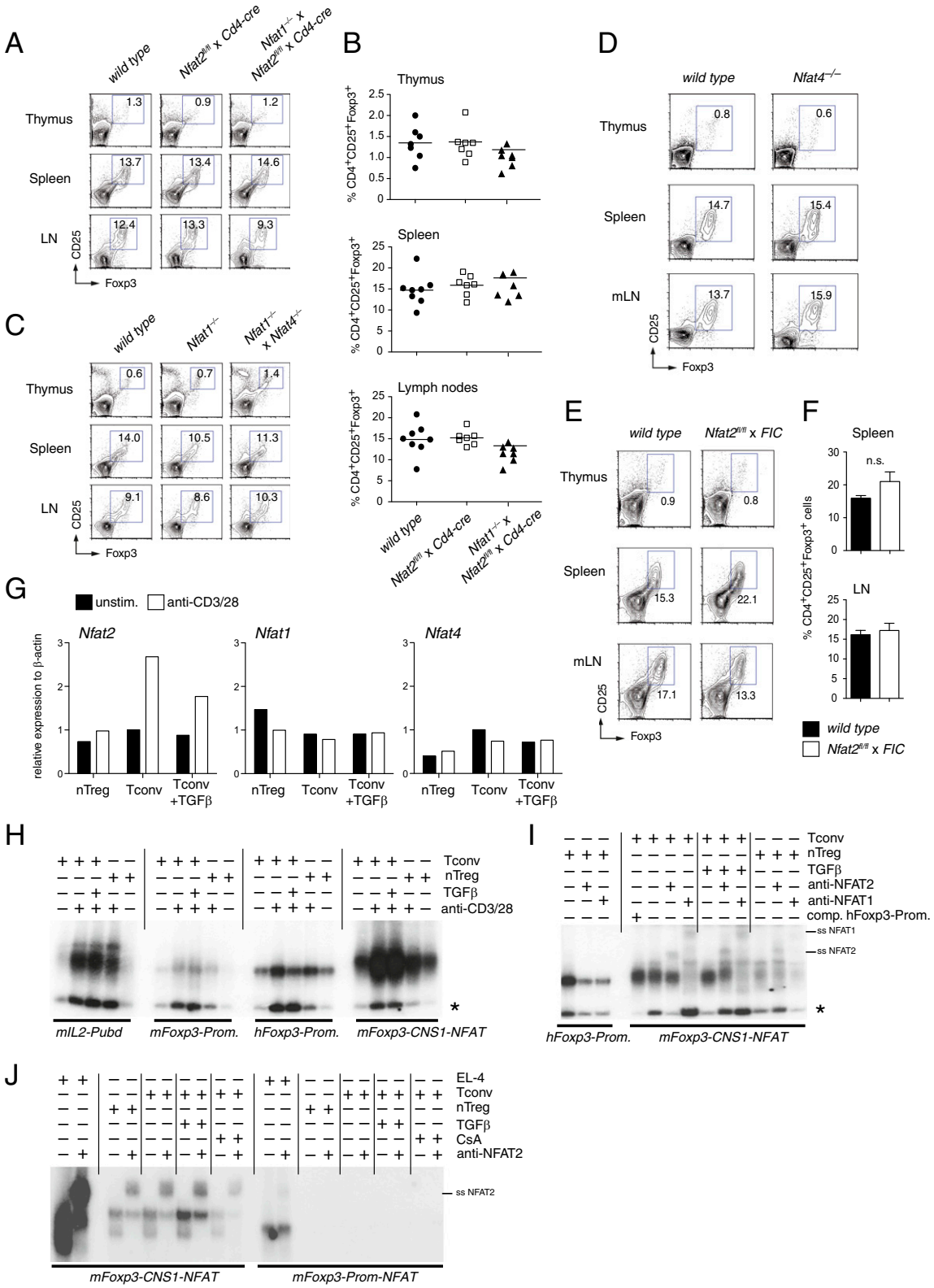

Fig. S3. Normal numbers of nTreg in NFAT-deficient mice. (*A* and *B*) *Nfat2*$^{fl/fl}$ × *Cd4-cre* and *Nfat1*$^{-/-}$ x *Nfat2*$^{fl/fl}$ × *Cd4-cre* mice show normal frequencies of CD4$^+$CD25$^+$Foxp3$^+$ nTreg in thymus, spleen, and LN. (*A*) Representative FACS analysis of gated CD4$^+$ cells and (*B*) synopsis of those from different lymphoid organs; each symbol represents one littermate. (*C*) Appearance of nTreg is unchanged in *Nfat1*$^{-/-}$ and *Nfat1*$^{-/-}$ × *Nfat4*$^{-/-}$ mice compared with WT. Flow cytometry of gated CD4$^+$ cells in thymus, spleen, and LN. (*D*) *Nfat4*$^{-/-}$ mice show normal frequencies of CD4$^+$CD25$^+$Foxp3$^+$ nTreg in thymus, spleen, and LN, representative FACS analysis of gated CD4$^+$ T cells. (*E* and *F*) Treg-specific deletion of *Nfat2* via *Foxp3-IRES-cre* (*FIC*) does not change the nTreg compartment. (*E*) Representative FACS determination of CD4$^+$CD25$^+$Foxp3$^+$ cells in thymus, spleen, and LN and (*F*) summary of four analyzed mice. (*G*) RNA of *Nfat1, Nfat2,* and *Nfat4* is expressed in unstimulated and anti-CD3/28–stimulated Tconv, nTreg, and Tconv in presence of TGF-β (iTreg induction), detected after 24 h by real-time PCR and normalized to β-actin. Human (*H* and *I*) and murine (*J*) nuclear protein extracts exhibit binding activity of NFAT1 and NFAT2 to *Foxp3-CNS1,* but hardly to the promoter (cells harvested for EMSA after 48 h; ss, supershift; *unidentified band).

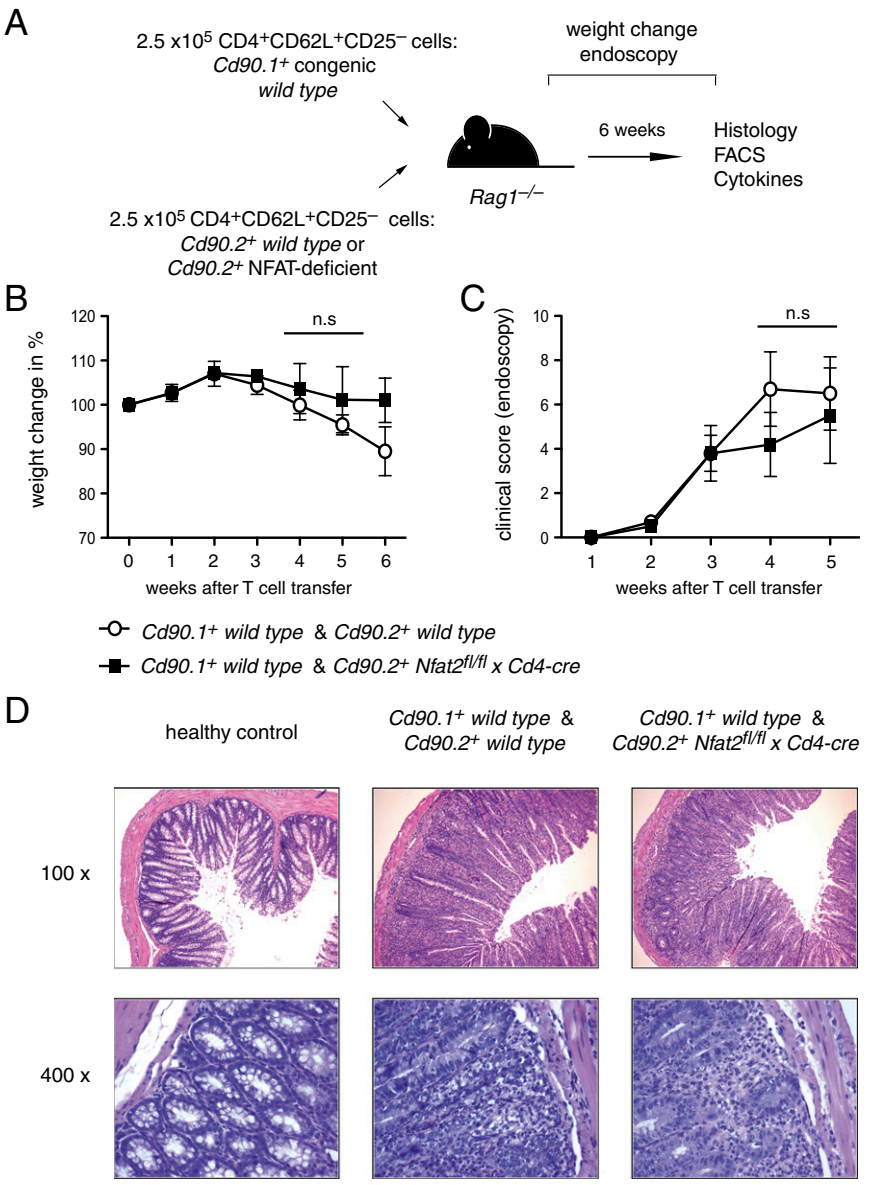

Fig. S4. Normal course of lymphopenia-induced colitis by NFAT2-deficient T cells. (*A*) Schematic overview of adoptive T cells transfer to induce colitis. 2.5×10^5 $CD90.2^+CD4^+CD62L^+CD25^-$ WT or NFAT-deficient T cells (*Nfat2*$^{fl/fl}$ × *Cd4-cre* or *Nfat1*$^{-/-}$ × *Nfat2*$^{fl/fl}$ × *Cd4-cre*) along with 2.5×10^5 $CD90.1^+CD4^+CD62L^+CD25^-$ congenic WT cells were injected i.p. into *Rag1*$^{-/-}$ recipient mice. (*B–D*) Normal course of colitis in *Rag1*$^{-/-}$ mice receiving NFAT2-deficient $CD4^+CD62L^+CD25^-$ T cells. (*B*) Monitoring weight change and (*C*) the clinical symptoms by colon endoscopy over 6 wk revealed only marginal differences in the characteristics of colitis in mice receiving either WT or *Nfat2*$^{fl/fl}$ × *Cd4-cre* T cells (five mice per group). (*D*) Representative H&E staining of paraffin-embedded colon sections showed no alteration of colitis in mice receiving either WT or *Nfat2*$^{fl/fl}$ × *Cd4-cre* T cells. As a reference a healthy colon (*Left*) in 100× and 400× magnification is given.

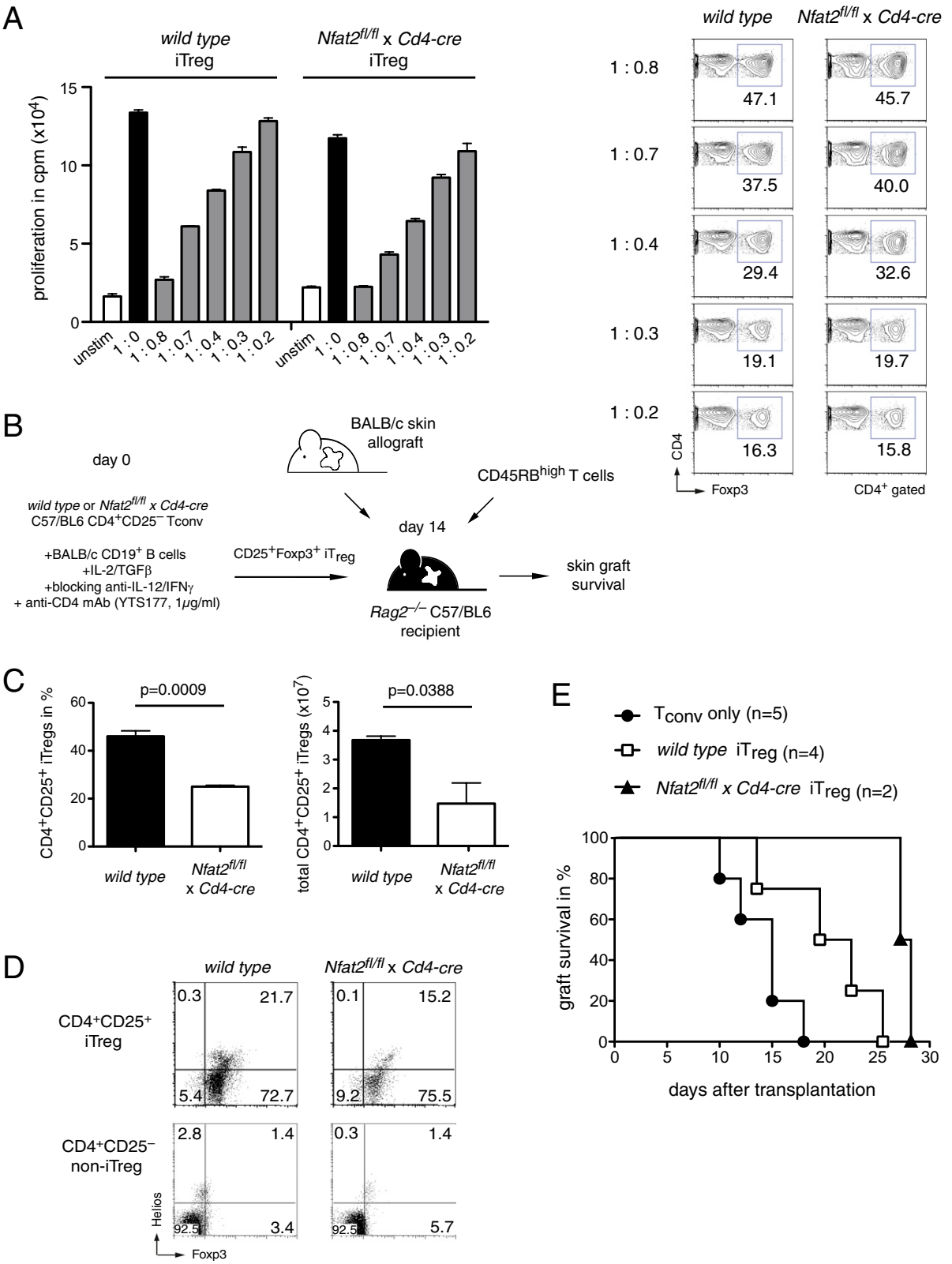

Fig. S5. Normal in vitro and in vivo suppressive capacity of NFAT2-deficient TGF-β–induced Treg. (*A*) CD4$^+$CD25$^-$ Tconv from WT and *Nfat2*$^{fl/fl}$ × *Cd4-cre* mice were stimulated for 3 d with anti-CD3/28 in presence of 5 ng/mL TGF-β followed by 12 d rest in medium containing IL-2 and TGF-β. CD25^{hi} cells were enriched and Foxp3 expression was analyzed by FACS. Different dilutions of Foxp3$^+$ iTreg (*Right*) were cocultured together with WT responder CD4$^+$CD25$^-$ T cells and APCs for 3 d. Ratio of responder vs. iTreg cells in culture is denoted (unstim, unstimulated 1:0.8 ratio as control). After 48 h proliferation was measured by thymidine incorporation (*Left*). Data are mean ± SD of triplicates. (*B–E*) NFAT2-deficient iTreg are fully suppressive in vivo. (*B*) Scheme of experimental setup to examine suppressive capacity of NFAT2-deficient iTreg in a model of allogenic skin transplantation. (*C*) CD4$^+$CD25$^-$ Tconv from WT and *Nfat2*$^{fl/fl}$ × *Cd4-cre* mice

Legend continued on following page

were cocultivated for 2 wk with allogenic BALB/c splenocytes in the presence of IL-2, TGF-β, anti-IL-12, and anti-IFNγ. Frequency of $CD4^+CD25^+$ allogenic-induced iTreg was controlled by FACS ($n > 5$). (*D*) Foxp3 and Helios expression of WT and $Nfat2^{fl/fl} \times Cd4\text{-}cre$ $CD4^+CD25^+$ iTreg from these cultures. (*E*) 2×10^5 WT or $Nfat2^{fl/fl} \times Cd4\text{-}cre$ iTreg depicted in *C* and *D* were injected along with 2×10^5 $CD4^+CD45RB^{hi}$ T cells i.v. in the $Rag2^{-/-}$ recipient mice and the BALB/c skin allograft survival was measured by log–rank test. All mice receiving only $CD4^+CD45RB^{hi}$ cells acutely rejected their skin transplants [$n = 5$, mean survival time (MST) = 15 d]. Addition of $Nfat2^{fl/fl} \times Cd4\text{-}cre$ iTreg prolonged skin graft survival as efficiently as WT $CD4^+CD25^+$ iTreg (WT: $n = 4$, MST = 22.0 d; $Nfat2^{fl/fl} \times Cd4\text{-}cre$: $n = 2$, MST = 27 d). Shown is one representative experiment out of two.

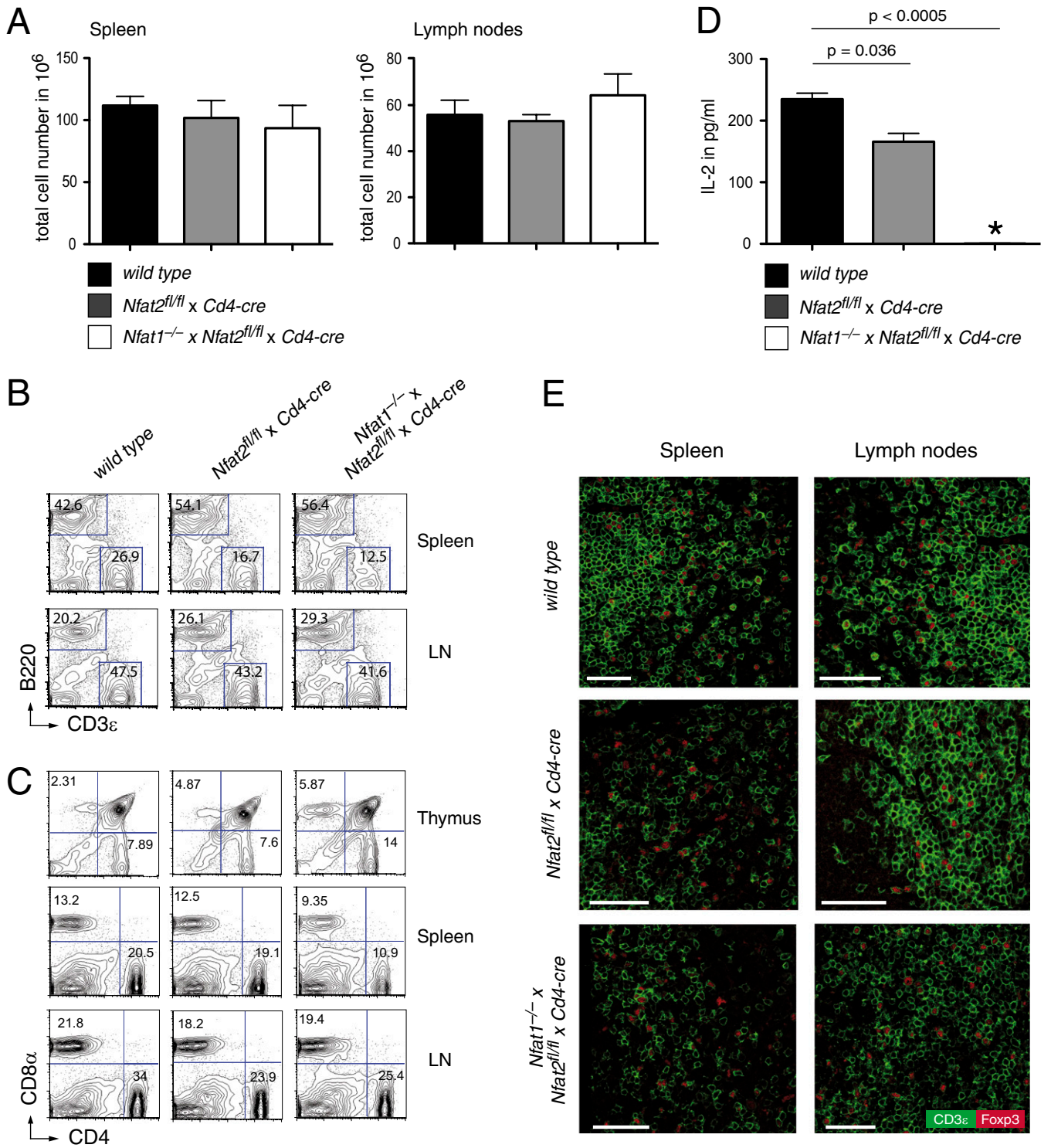

Fig. S6. NFAT-deficient mice display no evidence of autoimmune disorders. (*A*) Total cell numbers in spleen and LN of WT, *Nfat2*$^{fl/fl}$ × *Cd4-cre*, and *Nfat1*$^{-/-}$ × *Nfat2*$^{fl/fl}$ × *Cd4-cre* mice. Data are mean ± SD from at least six littermates. (*B*) Representative FACS analysis of B and T-cell compartments in spleen and LN of WT, *Nfat2*$^{fl/fl}$ × *Cd4-cre*, and *Nfat1*$^{-/-}$ × *Nfat2*$^{fl/fl}$ × *Cd4-cre* mice. (*C*) Frequency of CD4^{+} and CD8^{+} T cells in thymus, spleen, and LN of WT, *Nfat2*$^{fl/fl}$ × *Cd4-cre*, and *Nfat1*$^{-/-}$ × *Nfat2*$^{fl/fl}$ × *Cd4-cre* mice examined by flow cytometry. (*D*) Impaired IL-2 production by NFAT-deficient CD4^{+} T cells in vitro. Isolated CD4^{+}CD25^{-} Tconv from WT, *Nfat2*$^{fl/fl}$ × *Cd4-cre*, and *Nfat1*$^{-/-}$ × *Nfat2*$^{fl/fl}$ × *Cd4-cre* mice were stimulated with plate-bound anti-CD3/28 for 48 h, and produced IL-2 was assayed from supernatants by ELISA. Data are mean ± SD of triplicates done in one experiment and representative of two; asterisk denotes nondetectable levels of IL-2 in 100-fold diluted supernatants. (*E*) Paraffin-embedded section of spleen and LN from untreated WT, *Nfat2*$^{fl/fl}$ × *Cd4-cre*, and *Nfat1*$^{-/-}$ × *Nfat2*$^{fl/fl}$ × *Cd4-cre* mice were used for two color staining of Foxp3 (red) and CD3ε (green). (Scale bar, 80 μm.)

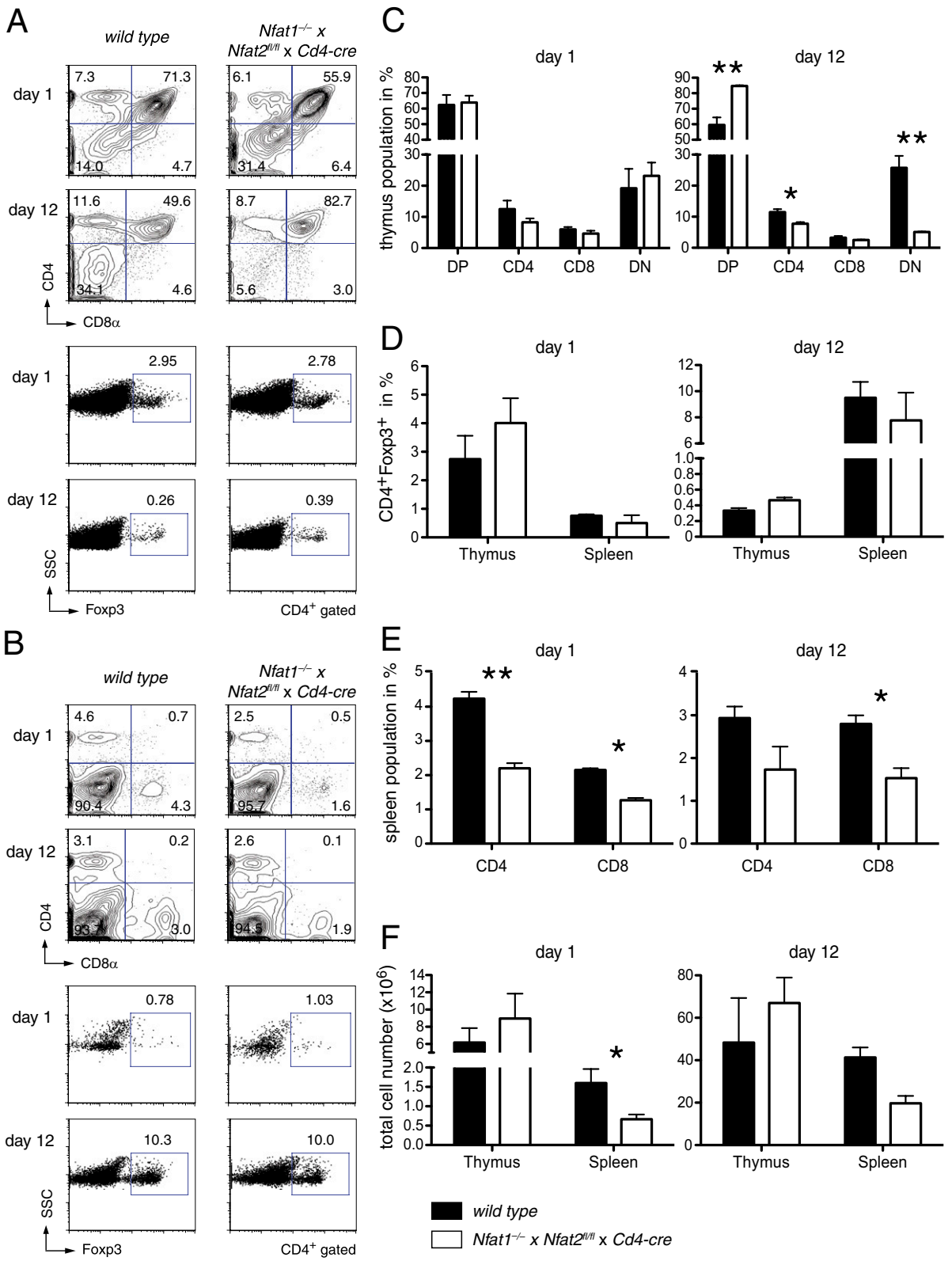

Fig. S7. Regular frequency of NFAT1 plus -2 double-deficient nTreg in newborn and young mice. (*A*) Representative FACS analysis of CD4/CD8 cell distribution (*Upper*) and nTreg frequency among CD4$^+$ cells (*Lower*) in the thymus of newborn and 12-d-old WT and *Nfat1*$^{-/-}$ × *Nfat2*$^{fl/fl}$ × *Cd4-cre* mice. (*B*) Representative FACS analysis of CD4/CD8 cell distribution (*Upper*) and nTreg frequency among CD4$^+$ cells (*Lower*) in the spleen of newborn and 12-d-old WT and *Nfat1*$^{-/-}$ × *Nfat2*$^{fl/fl}$ × *Cd4-cre* mice. (*C–F*) Quantification of at least three independent experiments shown as frequency in % (*C–E*) and total cell number (*F*) of thymus and spleen. *$P \leq 0.05$; **$P \leq 0.005$.

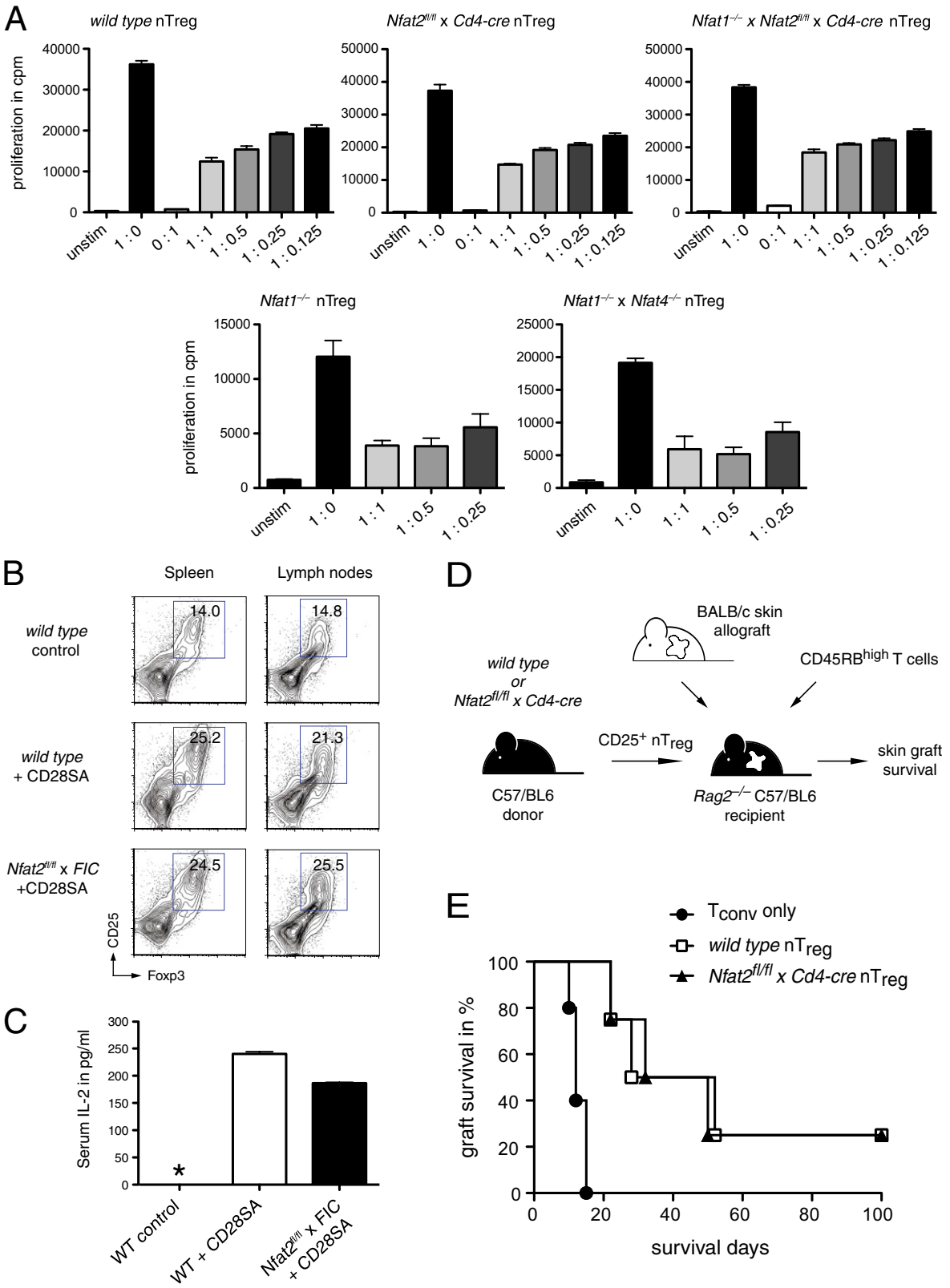

Fig. S8. NFAT-deficient nTreg exhibit normal suppressive capacities in vitro and in vivo. (*A*) $CD4^+CD25^+$ nTreg from WT, *Nfat2*$^{fl/fl}$ × *Cd4-cre*, and *Nfat1*$^{-/-}$ × *Nfat2*$^{fl/fl}$ × *Cd4-cre* (*Upper*) or *Nfat1*$^{-/-}$ and *Nfat1*$^{-/-}$ × *Nfat4*$^{-/-}$ mice (*Lower*) were stimulated together with WT responder $CD4^+$ T cells and APCs for 3 d. Ratio of responder vs. nTreg in culture is denoted (unstim, unstimulated 1:1 ratio as control). After 48 h proliferation was measured by thymidine uptake. Data are mean ± SD of triplicates done in one experiment and representative of four. (*B*) Frequency of *Nfat2*$^{fl/fl}$ × *FIC* nTreg is not impaired in spleen and LN of mice treated with 250 μg superagonistic CD28 mAb D665 (CD28SA) for 3 d. (*C*) Serum IL-2 was assayed by ELISA 2.5 h after CD28SA injection. Data are mean ± SD of triplicates. (*D* and *E*) NFAT2-deficient nTreg fully prevent skin allograft rejection in an adoptive transfer mouse model. (*D*) Schematic overview of adoptive

Legend continued on following page

transfer of B6 WT or *Nfat2*$^{fl/fl}$ × *Cd4-cre* CD4^{+}CD25^{+} nTreg along with CD4^{+}CD45^{hi} T cells into a B6 *Rag2*$^{-/-}$ recipient mouse, receiving a BALB/c skin allograft. (*E*) 5×10^5 nTreg along with 2×10^5 CD4^{+}CD45RB^{hi} cells were injected i.v. and BALB/c skin allograft survival in the *Rag2*$^{-/-}$ recipient mouse was measured by log–rank test. All mice receiving only CD4^{+}CD45RB^{hi} cells acutely rejected their skin transplants (n = 5, MST = 12.8 d). Addition of WT (n = 4, MST = 51.0) or *Nfat2*$^{fl/fl}$ × *Cd4-cre* Treg (n = 5, MST = 60.4) prolonged skin graft survival.

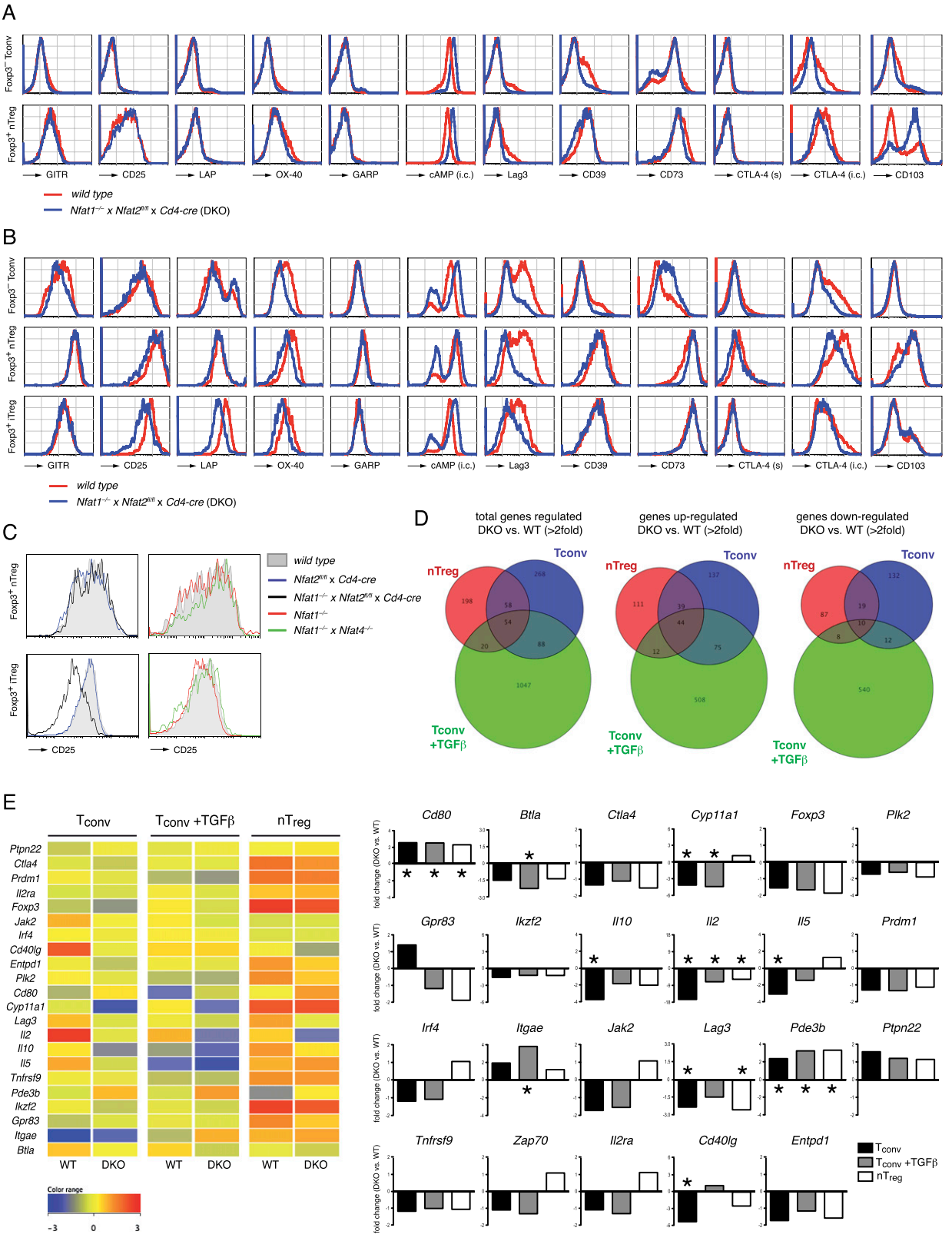

Fig. S9. Analysis of NFAT-deficient Treg on mRNA and protein levels. (*A* and *B*) Analysis of molecules involved in Treg-mediated suppression and homeostasis. (*A*) Freshly isolated splenic CD4$^+$ T cells from WT or *Nfat1*$^{-/-}$ × *Nfat2*$^{fl/fl}$ × *Cd4-cre* (DKO) mice were stained for indicated molecules. Subsequent intracellular Foxp3 staining identified nTreg and Tconv using FACS; i.c., intracellular; s, surface staining. (*B*) CD4$^+$CD25$^+$ nTreg and CD4$^+$CD25$^-$ Tconv from WT or *Nfat1*$^{-/-}$ × *Nfat2*$^{fl/fl}$ × *Cd4-cre* (DKO) mice were isolated and stimulated for 3 d with plate-bound anti-CD3/28 in absence (Tconv and nTreg) or presence (iTreg conditions) of TGF-β. Denoted molecules on Foxp3$^-$ Tconv, Foxp3$^+$ nTreg, or TGF-β–induced iTreg were analyzed by FACS. (*C*) Flow cytometry of CD25 expression in various NFAT-deficient Treg populations. CD4$^+$CD25$^+$ nTreg and CD4$^+$CD25$^-$ Tconv from WT, *Nfat2*$^{fl/fl}$ × *Cd4-cre*, *Nfat1*$^{-/-}$ × *Nfat2*$^{fl/fl}$ × *Cd4-cre*, *Nfat1*$^{-/-}$, and *Nfat1*$^{-/-}$ ×

Legend continued on following page

Nfat4$^{-/-}$ mice were isolated and stimulated for 3 d with anti-CD3/28 in the presence of TGF-β. After 4 d the CD25 expression on Foxp3^{+} nTreg and iTreg was measured by FACS. (*D* and *E*) Analysis of genes potentially regulated by NFAT:Foxp3-complexes using microarray gene profiling. (*D*) Venn diagram illustrations of genes regulated more than twofold between *Nfat1*$^{-/-}$ × *Nfat2*$^{fl/fl}$ × *Cd4-cre* (DKO) and WT in CD4^{+}CD25^{+} nTreg and CD4^{+}CD25^{-} Tconv stimulated for 24 h with anti-CD3/28 in presence (Tconv+TGF-β, iTreg polarizing conditions) or without TGF-β (nTreg and Tconv). Data represent two completely independent biological experiments. (*E*) Representation of suggested NFAT:Foxp3-regulated genes in DKO and WT nTreg, Tconv, and Tconv+TGF-β stimulated for 24 h with anti-CD3/28 as heatmap (*Left*) or bar graphs (*Right*). Clustering analysis and heatmap of expression values show the log2 transformed expression intensity of the genes. Genes regulated ≥twofold between DKO and WT are tagged with an asterisk. Data from two independent biological experiments are given as an average of reliable entities representing denoted genes.

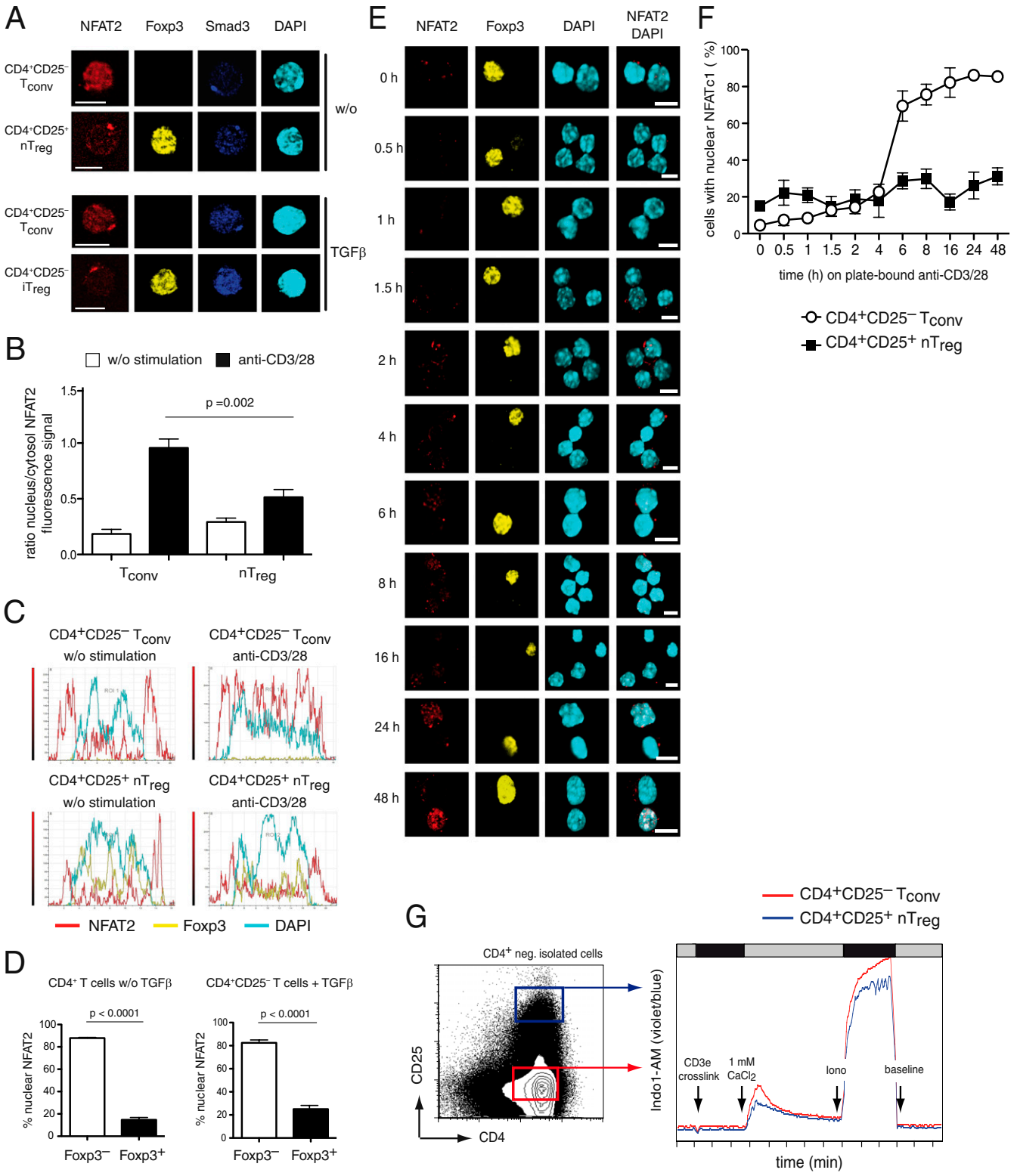

Fig. S10. Impaired nuclear translocation of NFAT2 in Foxp3$^+$ cells. (*A* and *B*) Four-color staining of NFAT2 (red), Foxp3 (yellow), Smad3 (blue), and chromatin (cyan) of freshly isolated CD4$^+$ conventional T cells (Tconv) and CD4$^+$CD25$^+$ nTregs stimulated for 6 h with anti-CD3 and anti-CD28 (*Upper*). Foxp3$^-$ Tconv and TGF-β-induced Foxp3$^+$ iTregs generated from CD4$^+$CD25$^-$ Tconv after 24 h stimulation with anti-CD3 plus anti-CD28 (*Lower*). (*B*) Quantification of nuclear and cytosolic fluorescence signal of NFAT2 in freshly isolated CD4$^+$ Tconv and CD4$^+$CD25$^+$ nTregs by confocal microscopy, nuclei were demarcated by DAPI staining. The ratio of nuclear/cytosolic signal was calculated of unstimulated (w/o) and 6 h anti-CD3/CD28 stimulated cells, data are mean ± SEM from at least 100 cells out of three individual experiments. (*C*) Histograms of one representative Foxp3$^-$ Tconv and nTreg cell, respectively, show different NFAT2 nuclear translocation after 6 h stimulation by anti-CD3/28. Red line represents NFAT2 staining, yellow line Foxp3, and the nucleus is demarcated by cyan DAPI staining. (*D*) Quantification of cells with nuclear NFAT2 in CD4$^+$ Tconv and CD4$^+$CD25$^+$ nTreg (*Left*) and 24 h TGF-β–induced Foxp3$^+$ iTreg (*Right*), data are mean ± SEM

Legend continued on following page

from more than 100 cells out of four individual experiments. (*E* and *F*) $CD4^+$ T cells were stimulated with plate-bound anti-CD3/28 for the indicated time points, and NFAT2 nuclear translocation was recorded using confocal microscopy. Representative pictures (*E*) and the quantification of more than 30 individual cells (*F*) are shown. (*G*) Calcium-influx measurement in $CD4^+CD25^-$ Tconv (red line) and $CD4^+CD25^+$ nTreg cells (blue line) by real-time flow cytometry. $CD4^+$ T cells were loaded with calcium-sensitive dye Indo1-AM and stained subsequently with anti-CD25-PE and biotinylatd anti-CD3ε. After 1 min the CD3ε Abs were cross-linked with streptavidin followed by the addition of 1 mM $CaCl_2$ after 3.5 min. As a positive control Iono was added after 9 min of measurement, as a negative control nonactivated cells were analyzed again as a baseline after 12 min.